A thermo-economic assessment of CSP+TES in the north of Chile for current and future grid scenarios

Cite as: AIP Conference Proceedings **2126**, 030023 (2019); https://doi.org/10.1063/1.5117535
Published Online: 26 July 2019

Felipe Gallardo, Luca Pratticò, and Claudia Toro

A Thermo-Economic Assessment of CSP+TES in the North of Chile for Current and Future Grid Scenarios

Felipe Gallardo[1,2, a)], Luca Pratticò[3, b)], Claudia Toro[3, c)]

[1] *Solar Committee of Chile (Comité Solar), Agustinas 640, 8320219 Santiago, Chile.*
[2] *DIAEE, University of Rome "Sapienza", Via Eudossiana 18, 00184 Rome, Italy.*
[3] *DIMA, University of Rome "Sapienza", Via Eudossiana 18, 00184 Rome, Italy.*

[a)]Corresponding author: felipeignaciogallardo@gmail.com
[b)]luca.prattico@uniroma1.it
[c)]claudia.toro@uniroma1.it

Abstract. This paper presents a thermo-economic analysis of a hypothesized concentrated solar power (CSP) tower plant with molten salt thermal energy storage (TES) located in the Atacama Desert in Chile with the aim of serving as input for the Solar Committee to better establish public policy programs to increase the competitiveness of CSP in Chile. The study focuses on an optimal plant in terms of size and configuration for expected conditions of the Chilean electricity market in 2018 and 2030. An ideal CSP+TES configuration to complement the electricity pool market from a grid point of view was obtained for each year. An exergetic study was performed for each configuration under assumed annual operation conditions and a thermos-economic analysis was done considering specific costs per component. Thermo-economic indicators were obtained allowing to define a priority hierarchy of specific techno-economical improvements that can be done at plant and component level to maximize the competitiveness of CSP projects in the Chilean market. A sensitivity analysis was performed obtaining the impact of efficiency improvements and capex reductions per component on the Levelized Cost of Energy (LCOE). The maximum allowable trade-off limit for each technical improvement (capex increase or plant factor reduction) was calculated.

INTRODUCTION

The Atacama Desert in the North of Chile is the region with the highest solar radiation in the world (DNI >3500 kWh/m^2 year) [1] and it is the center of the most intensive copper mining region of the planet with a consequent high energy demand and flat hourly profile [2]. It also represents a key entrance for Chile to South America as it limits with Argentina, Bolivia, Peru.

These conditions combined with a favorable public policy and a clear regulation in the electricity market, have led the country into a successful deployment of wind plants along the country (1,305 MW), and of PV plants (1,852 MW) particularly in the Atacama Desert during the last decade[3]. Nevertheless, the introduction of these technologies has created new requirements in the grid, to supply peak and base load demand at a competitive price while keeping a low carbon emission factor. The Economic Development Agency of Chile, *CORFO*, through its dedicated Solar Committee, *Comité Solar*, has promoted the development of Concentration Solar Tower Power Plants "STPP" with Thermal Energy Storage "TES" plants in the Atacama Desert as the most suitable technology to supply electricity according to the needs of the industry, while creating conditions to deploy a local CSP industry of goods, services and human resources[4].

Many works have evaluated the power cycles performance using energy, exergy or thermo-economic analysis [5] but only few works have focused on STPP. Xu et al [6] analyzed a basic design of STPP with no energy storage system and a re-heated Rankine cycle showing that the maximum exergy loss occurs in the receiver system and the heliostats field. Other works focused on different improvements like the use of Kalina cycle [7] or an hybrid cogeneration cycle [8]. However, no thermo-economic approach was applied in these works. Only [9] and [10] performed a thermo-

SolarPACES 2018
AIP Conf. Proc. 2126, 030023-1–030023-10; https://doi.org/10.1063/1.5117535
Published by AIP Publishing. 978-0-7354-1866-0/$30.00

economic analysis on STPP. The first analyzed a 1.4MW plant that employs air as the Heat Transfer Fluid "HTF" in the receiver showing in their results that the conventional combined cycle present better performance than other options. The second investigated the influence of the steam generator pinch point in a 110MW STPP obtaining an optimum pinch point that minimizes exergy destruction.

This paper focuses on finding the most suitable opportunities to optimize the cost of the CSP tower components to be developed in the conditions of the Atacama Desert and the electrical grid of Chile from a thermo-economic point of view.

Identification of Optimal CSP + TES Configurations

To perform a thermo-economic analysis, it is mandatory to recognize the cost-contribution of each component of the CSP plant to the cost of electricity. This cost-contribution varies for different projects of the same technology due to sizing, operation or primary resource availability among other factors, therefore a case of study must be selected. The present study considers as case of study a specific configuration of CSP tower with molten salt TES of 110 MWe operating in the Chilean electrical system for which two scenarios, current (2018) and future (2030), were considered. The location was selected to be *Diego de Almagro* in the Atacama Desert [1] whose solar resource and weather conditions input data have been largely studied by the Solar Committee.

The specific configuration and size of the case of study are obtained for each scenario by simulating the hourly optimal dispatch of 300 configurations with SAM [2] considering solar multiples "SM" from 1 to 3.5 and hours of storage from 1 to 19. The solar field (receiver dimensions, heliostat field layout and tower height) was optimized for each SM value and specific CAPEX and OPEX were considered for each scenario[11].

The selected configuration for each scenario is selected by a simple techno-economic analysis, obtaining the most competitive design within the centralized market of Chile in each year. Particularly, the selected configuration is which maximizes the net profit considering total investment values and Spot and PPA performances as shown in Eq 1.

$$\mathrm{Spot}_{perf} = \sum_{i}^{n} \mathrm{Gen}_i \bullet (\mathrm{Spot}_{price_i}^{injection} - \mathrm{CSP}_{varcost\,i}) \;;\; \mathrm{PPA}_{perf} = \sum_{j}^{n} \mathrm{Demand}_j \bullet (\mathrm{PPA}_{price_j} - \mathrm{Spot}_{price_j}^{withdrawal}) \qquad (1)$$

The hourly spot price was considered exogenous and it was obtained from real market data from the ISO *Coordinador Eléctrico Nacional* "CEN" for the 2018 [12] while for the 2030 scenario it was obtained from the official national long-term energy plan or "PELP" by the Ministry of Energy of Chile [12]. The PPA price was assumed to be the average market price obtained from the regulator *Comisión Nacional de Energía* "CNE" public data [13].

Current and future scenarios specifics costs were defined considering CSP cost reductions expected by regulator, and expected operation and spot prices of the market according to the long-term energy plan, by the Chilean Energy Ministry [12] as shown in Tab. 1. As it is necessary, for the later thermoeconomic analysis, to divide the total cost of the plant to the considered components, general not component cost such as Engineering, Procurement and Construction (EPC) where proportionally charge to the CAPEX of the components, while complex components cost, such as heliostat field, represents the sum of costs of more than one subcomponent, eg, land, and heliostat field itself.

TABLE 1. Specific cost by component for current and future scenarios (without EPC).

Scenario	Heliostat field [US$/m2]	Receiver [MMUS$]	TES [US$/kWt]	Steam generator [US$/kWe]	Power block [US$/kWe]
2018	178	63.8	24	350	1100
2030	96	39.1	15	200	750

The identified most efficient configurations for each scenario are reported in Tab. 2 where the *market performance* parameter is defined as the ratio between total annual expected revenue and the annuity of the total cost.

TABLE 2. Optimal CSP configurations

Scenario	Solar multiple	Hours of TES [h]	Total cost [MMUS$]	LCOE [US$/MWh]	Plant factor	Market performance
2018	2.9	14h	710.4	65.6	83.9%	72.5%
2030	2.5	12h	385.4	48.1	73.5%	132.5%

METHODOLOGY

Exergy Content Calculation

Once the preliminary techno-economic assessment is completed, exergy content per stream and the exergy destruction per component might be calculated. To do so, the power plant has been modeled as an interconnected set of components. Each component will stand a certain number of input and output streams with specific exergetic content. In Tab. 3, the component decomposition of the plant is shown.

TABLE 3. CSP components and exergy streams

Component	Inputs streams	Output streams
Cold Tank (CT)	Cold molten salt (from SG)	Cold molten salt (to Rec)
Tower/Receiver (rec)	Cold molten salt (from CT) Electricity to pump (from PB) Concentrated irradiation (from HF)	Hot molten salt (to HT)
Heliostat field (HF)	Solar irradiation (from sun)	Concentrated Irradiation (to rec)
Hot tank (HT)	Hot molten salt (from Rec) Electricity to pump (from PB)	Hot molten salt (to SG)
Steam generator (SG)	Hot molten salt (from HT) Cold water (from PB)	Cold molten salt (to CT) High pressure steam (to PB)
Power Block (PB)	High pressure steam (from SG)	Electricity (final product) Condensate water (to SG)

The exergy content of a substance or a stream is defined as the maximum amount of work that can be obtained when the stream is brought from its initial state "S" to the dead state "O" [14] by processes during which the stream may interact only with the environment. Exergy represents a measurement of the energy quality in terms of usefulness to perform work [15]. As energy and work, exergy can be obtained in several different forms and therefore the exergy content calculation will depend on the type of work that can be performed, on the "S" and "O" states [15]. The exergy content of a substance can be thermal, chemical, mechanical, kinetic or potential.

In this paper, the thermal exergy content, and the exergy of electricity are considered as the other kinds can be neglected for the aim this study. The exergy calculation considered per stream is shown in the Eq. 2, 3, 4 and 5.

$$\text{Exergy}_{\text{solar irradiation}} = Q_{\text{sun}} \bullet \left(1 - \frac{T_o}{T_{\text{sun}}}\right) \tag{2}$$

where T_{sun} is the apparent sun temperature as an exergy source and taken to be 4500 K [16].

$$\text{Exergy}_{\text{molten salt}} = H_{\text{molten salt}} - H_{\text{molten salt}_o} - T_o \bullet (S_{\text{molten salt}} - S_{\text{molten salt}_o}) \tag{3}$$

$$\text{Exergy}_{\text{water}} = H_{\text{water}} - H_{\text{water}_o} - T_o \bullet (s_{\text{water}} - s_{\text{water}_o}) \tag{4}$$

$$\text{Exergy}_{\text{electricity}} = \text{Energy}_{\text{electricity}} \tag{5}$$

For the aim of this study, the chosen thermodynamic reference environmental state was a temperature of 298 K and pressure of 101.325 kPa, all the specific operation temperature and pressure per stream were extracted from SAM simulations while specific properties of enthalpy and entropy were obtained using the CoolProp library [17]. In this manner, the exergy content for each stream are obtained.

It is important to highlight that, as the mass flows and profiles of hourly operation are different for each stream, to perform a correct thermoeconomic analysis the exergy content must be considered hourly, otherwise the input/output balance would not be respected.

Finally, the exergy waste, defined as the addition of normal exergy losses (for example due to non-ideally adiabatic processes) and exergy destruction, due to irreversibilities (for example the reduction on temperature) can be calculated as the difference between exergy inlet and outlet for each the component.

Thermoeconomic Cost Calculation

The specific thermoeconomic cost per stream, defined as the unit cost of exergy [US$/kJ] , can be calculated by solving the annualized cost balance equations per component [16].The resultant equation system based on the application of Eq.6 to the components is underdetermined as there are more streams (9 variables) than components (6 equations). 3 auxiliary equations are needed. The first 2 auxiliary equations (Eq. 7 and 8) are border conditions related to the free cost of solar irradiation and the waste consideration of cold water out of the condenser. The third auxiliary equation (Eq. 9) is obtained by using the Extraction Method [16] on the molten salt before and after the steam generator.

$$c_{fuel} \bullet Ex_{fuel} - c_{product} \bullet Ex_{product} - Zc = 0 \tag{6}$$

$$c_{solar\ irradiation} = 0 \tag{7}$$

$$c_{cold\ water} = 0 \tag{8}$$

$$c_{hot\ molten\ salt} = c_{cold\ molten\ salt} \tag{9}$$

The capital cost rate Z_c [US$/h] by component, is obtained considering the capex, a horizon of 20 years, a WACC of 5% and the respective plant factors PF for each scenario as it shown in Eq. 10.

$$Z_c = \frac{Z_{component} \bullet CRF}{PF \bullet 8760} \tag{10}$$

The resultant system can be written and solve as a matrix system of the form expressed in Eq. 11.

$$A_{(9x9)} \bullet c_{(1x9)} = -Z_{(1x9)} \tag{11}$$

Thermoeconomic indicators

A direct way to establish a hierarchy of components that should be attend more importantly to achieve an overall optimization of the plant is by evaluating the thermoeconomic indicators of relative added value factor and exergoeconomic factor, both defined per component [16].

- The **"Relative added value" (**Eq. 12) represents the relative increase in average cost per exergy unit between fuel and product. Whenever there are components with more than one inlet or outlet, a weighted average cost is considered. Components with a high Relative added value factor are to be evaluated first.

$$R_{added\ value} = \frac{c_{product} - c_{fuel}}{c_{fuel}} \tag{12}$$

- The **"Exergoeconomic factor"** (Eq. 13) expresses as a ratio, the contribution of the non-exergy related cost to the total cost increase. A low value of the exergoeconomic factor calculated for a major component suggests that cost savings in the entire system might be achieved by improving the component efficiency even if the capital investment cost for this component will increase. On the other hand, a high value of this factor suggests a decrease in the investment costs of this component at the expense of the components efficiency.

$$Exergo_{factor} = \frac{Z_c}{c_{waste} \bullet Ex_{waste} + Z_c} \tag{13}$$

Sensitivity Analysis

A sensitivity analysis on the LCOE is done by considering actions that might result in overall efficiency improvements for the CSP plant based on the thermoeconomic indicators obtained. The maximum allowable trade-off for those actions is studied.

RESULTS

The specific thermoeconomic cost of exergy per stream as shown in Fig.1 shows that the thermoeconomic cost of the net produced electricity is 65.6 US$/MWh for 2018 while a strong reduction is seen for 2030 with 48.1 US$/MWh due to both reduction in capex and change of configuration. The results shown that the specific cost is smaller for high exergy content streams, such as heliostat field outlet or receiver, while comparatively low exergy content streams such as cold tank outlet and net produced electricity have higher specific cost values (condensate water and solar irradiation are supposed to have null specific cost). It is therefore noticed that whether a high exergy destruction or an improvable capex is expected in the receiver component, between the heliostat field and cold tank outlets and the receiver outlet, as there is a strong increment in the specific cost even though the mass flow rate of charging molten salt it is the constant.

On the other hand, specific cost differences are noticed between inlet and outlet streams in the storage tanks due to the integrated consideration of the molten salt pumps as integral part of the tanks therefore the storage tank outlets are higher due to the exergy increment added by the evacuation pumps with a notorious more marked effect on the cold tank which is connected to the receiver above the tower. The dramatic increase in the electricity specific cost with respect to the high-pressure steam specific cost is due to the low second law efficiency of the power block, and mainly the turbine.

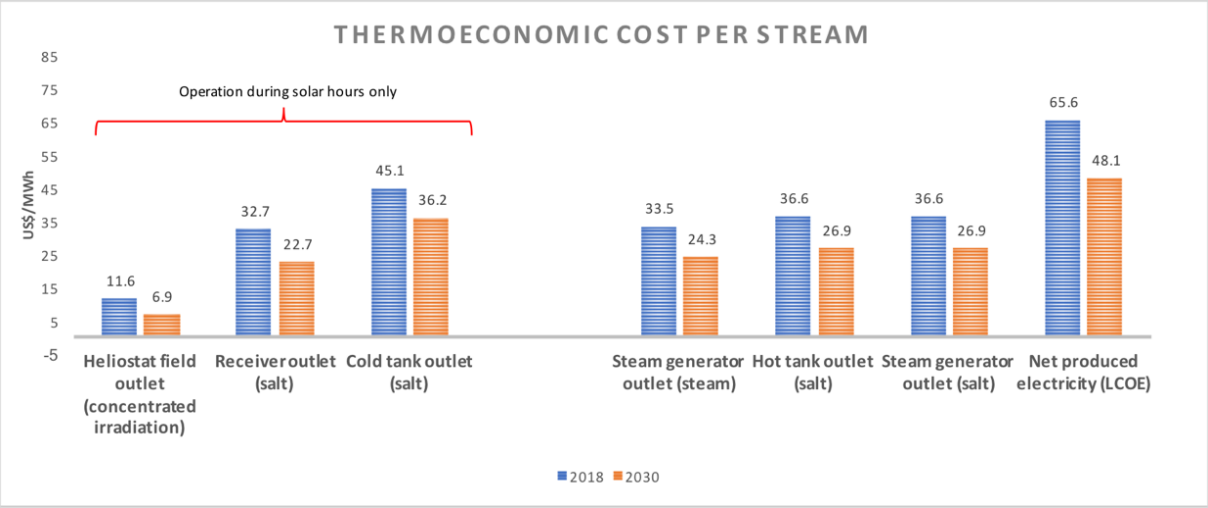

FIGURE 1. Thermoeconomic cost per stream of each component for 2018 and 2030

The pattern of cost composition per stream does not change with the year of study as expectable as there are no supposed efficiency increments and all the components reduce their capex in a proportional manner to 2030.

The thermoeconomic factors shown in Fig. 2 confirm the higher relative added value of the receiver which comes along with a low exergoeconomic factor, implying that the added value is not strongly sensitive to the capex but to the efficiency and that there is still space to implement improvements in efficiency even at high cost for this component. For both factors on this component, a negligible reduction is seen for 2030.

The relative added value factor of the heliostat field is infinite due to free cost of fuel, solar irradiation, and therefore is not shown in Fig. 2, Nevertheless, the exergoeconomic factor of this component is the highest of the group and so it implies that heliostat field improvements on capex are expected to be more effective than on efficiency. This insight is not necessarily extendable to other components with high exergoeconomic factors.

The hot tank and steam generator and the cold tank respectively present the lowest relative added values due to the high values of the fuel that must handle. In the case of the steam generator, the factor is somehow distorted by the auxiliary equations on its molten salts streams making the cost of the fuel be close to the cost of the product and consequently causing the relative added value to be low.

From the observation of this factors, the improvements actions were chosen in first place to improve the efficiency of the receiver through the usage of a wider range of work temperature for the molten salt and receiver efficiency itself, in second place improvements regarding the heliostat field and finally the steam generator. Improvements

actions on the power block were dismissed as this study considered a power block based on rankine cycle only and it is a mature technology.

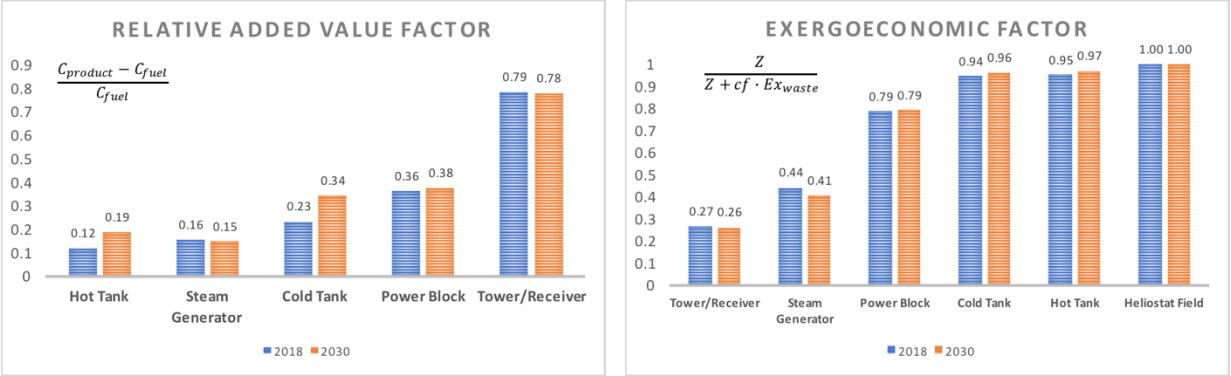

FIGURE 2. Thermoeconomic indicators: Relative added value factor and Exergoeconomic factor for 2018 and 2030

A ceteris paribus sensitivity analysis is performed on the cost of the net electricity calculated by means of the thermoeconomic analysis, which in time, as the exergy content of electricity is equal to its energy content is equivalent to the LCOE without prejudice that LCOE method implies a whole different calculation mechanism [18]. A set of actions to reduce the LCOE, shown in Tab. 4, was considered for the sensitivity analysis.

TABLE 4. Improvement actions for LCOE sensitivity analysis

Group of actions	Actions	baseline	3%	6%	9%	12%
Operational improvements	High Temp. of salt [K]	847	872	898	923	949
	Low Temp. of salt [K]	563	546	529	512	481
	Heliostat Field eff. [%]	86%	88%	91%	93%	99%
	Receiver eff. [%]	87%	90%	92%	95%	97%
	Steam Generator eff. [%]	88%	91%	93%	96%	99%
Capex reduction 2018	Receiver [MMUS$]	74	72	69	67	65
	Heliostat Field [MMUS$]	284	275	267	258	250
	Steam Generator [MMUS$]	45	43	42	41	39
Capex reduction 2030	Receiver [MMUS$]	44	42	41	40	38
	Heliostat Field [MMUS$]	146	142	138	133	129
	Steam Generator [MMUS$]	25	24	23	22	22

The actions were chosen accordingly with the results of the thermoeconomic analysis Fig. 1 and thermoeconomic indicators Fig. 2. Two groups of improvement actions are considered: operational improvements actions and capex reductions actions, for which, the whole previous procedure is reapplied and so the exergetic costs and factors are reobtained for each case. The improvements actions, described were obtained by proposing improvements of 3%, 6%, 9% and 12% whether for efficiency improvements or for capex reductions, applied to the baseline initial considered values. In the case of capex reductions and low temperature of molten salts, the variations are of course negative with respect of the baseline value, with the aim of obtaining an improvement on the performance of the plant.

The LCOE sensitivity analysis shows that the most efficient way to reduce the cost of the produced electricity is to improve the efficiency of the steam generator independent of the year of study with an average percentage reduction on the LCOE almost equal to the percentage increment on the efficiency of this component.

The steam generator achieves the transfer of exergy from molten salt to water, therefore it is the last component before the power block. As the principle of exergy destruction guarantees that the exergy content will reduce from one component to the next, any efficiency improvement on a component will cause, in principle, more impact if it is done as close as possible to the component whose outlet is the final product as it is seen in Fig 3 where after the steam

generator, for 2018 the next most efficient improvement is achieve by increasing the efficiency of the receiver followed by a reduction on the capex of the heliostat field. However, this corollary is not infallible as does not take into account the cost of the components. In fact, for 2030 a change within the most efficient actions to improve LCOE is seen, where the temperature of molten salt, in any case related to the efficiency receiver, have more impact.

Despite being the most sensible component affecting the LCOE for both 2018 and 2030, it is shown in Fig. 3 that a reduction in capex for the steam generator would have a negligible impact on LCOE, allowing to distinguish that given a critical component for the cost composition of the plant, does not imply that any action would be effective on it to improve competitiveness, moreover if the action does not address the correct aspect, it could result in null effect. In fact, it is important to notice that also in the case of receiver, as predicted by the observation of thermoeconomic factors, the most efficient action for improvement is related to an efficiency increment while for the heliostat field it is related to a capex reduction for both years of study.

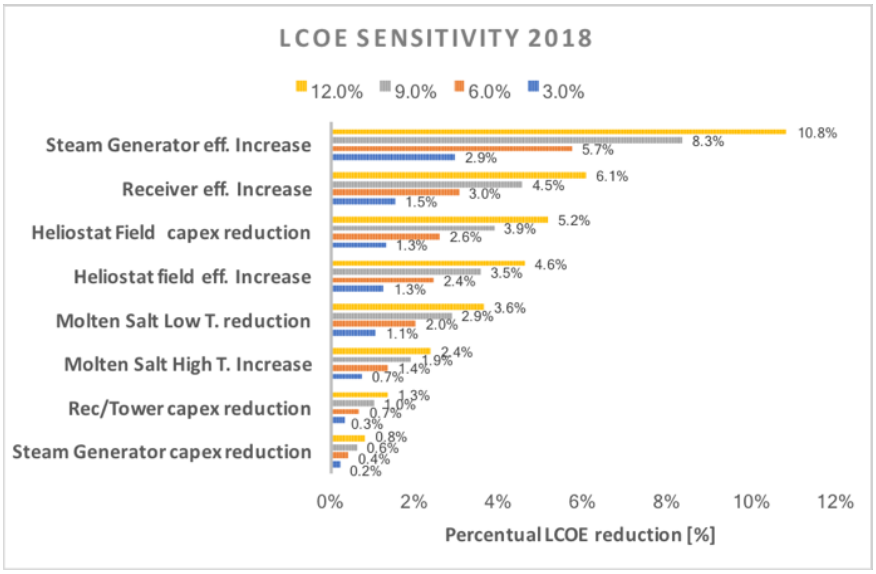

(a)

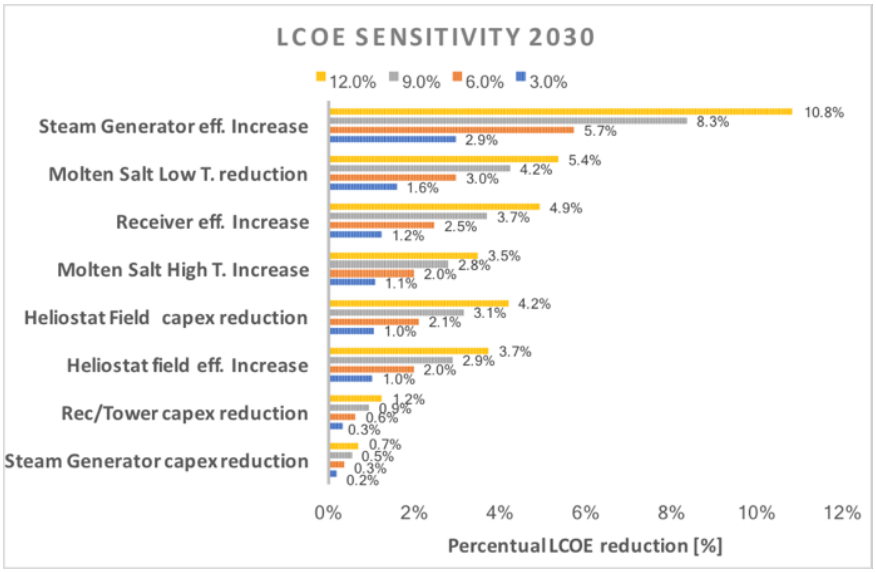

(b)

FIGURE 3. LCOE sensitivity for 2018 and 2030

Whenever an efficiency improvement is to be obtained for a given technology, there is usually a trade-off in terms of cost, while efforts to reduce the capex might often implied a compromise in efficiency. These trade-offs are analyzed in this paper establishing for each improvement action, the maximum cost increase or plant factor variation that would maintain the LCOE in the baseline level. Whenever an operational improvement costs more than the limit, then the action it would result in a net increase of the LCOE, therefore it is not advisable. On the other hand, if a capex reduction action results in a reduction of the plant factor, higher than the trade-off limit, the action would not be advisable as an improvement neither. Fig. 4 and 5 show these maximum trade-offs that might be accepted for the proposed actions.

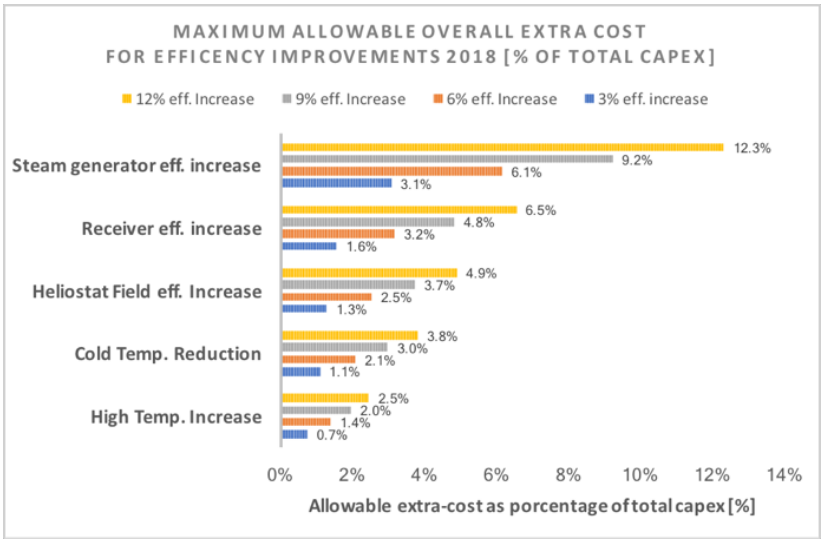

(a)

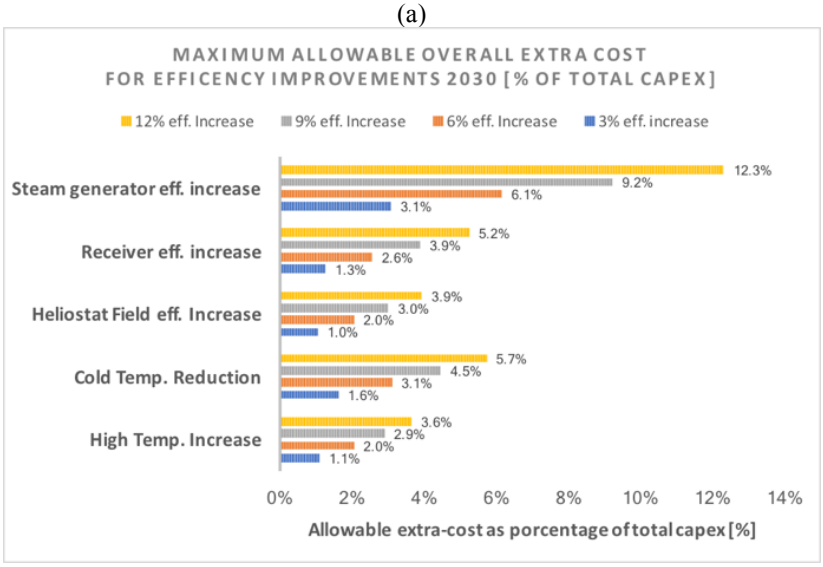

(b)

FIGURE 4. Maximum allowable extra cost for efficiency improvements for 2018 and 2030

As expected, Fig. 4 shows that the actions with a higher impact on the LCOE are the ones that allow a higher increment of the CAPEX. It is important to highlight that the limit of total capex increment for an increment in the steam generator efficiency is higher than 1% of the total capex per a 1% increment in the efficiency for both 2018 and 2030, which is far more than the limit for other operational improvement actions, practically doubling the next most

efficient action in each year. The lowest impact obtained is for the increment of high temperature of the molten salt for both years while the reduction of temperature in the cold molten salt appears to have more margin in terms of the cost that would implied to be achieve, specially in 2030 when the overall cost of the plant is reduced.

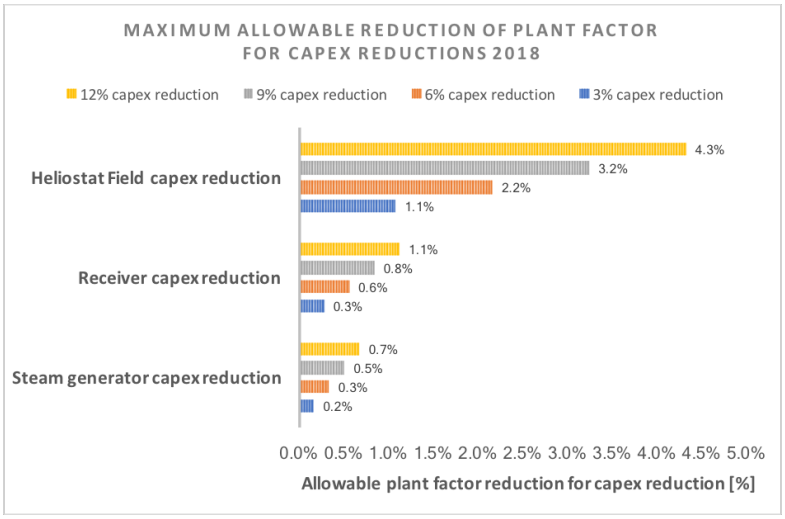

(a)

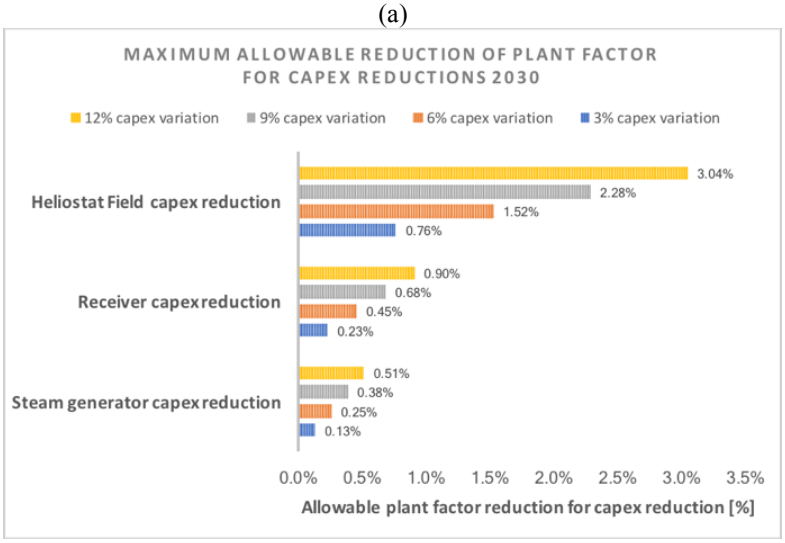

(b)

FIGURE 5. Maximum allowable plant factor reduction for capex reduction for 2018 and 2030

As shown in Fig. 5, the plant factor reduction limit also behaves according to the impact of the actions on the LCOE. Notorious is the case of the heliostat field in 2018, where the relation between 1 point of capex reduction on the component, can be profitable even for a reduction of the plant factor of around 0.3 points. This group of actions reduces its trade-off limit for 2030 due to cost reductions, however the reduction of the limit does not vary strongly.

CONCLUSIONS

The thermoeconomic analysis performed on optimal selected configurations of CSP tower plants in the Atacama Desert shows that the most critical components in terms of added value are the heliostat field and the receiver, however, exergoeconomic factor analysis shows that improvements in efficiency are more important than cost reduction for the receiver while for the heliostat field is the opposite.

Projected cost reductions and change in grid scenarios between 2018 and 2030 cause a change in the expected optimal configuration of CSP towers in Chile, nevertheless the hierarchy of thermoeconomic cost composition per stream and relative added value per component remains the same, implying that improvement challenges are long term task even if cost reduction projections are achieved.

For the current scenario, the most effective action to reduce cost of electricity among the studied actions is to increase the efficiency of the steam generator, to increase the efficiency in the receiver and to reduce the capex of the heliostat field respectively. This last action might be a low hanging fruit to promote competitiveness of CSP in Chile, as it might represent a technologically simpler task than the first two.

If cost projections are achieved for 2030, the low operational temperature of the molten salt appears to be of higher importance than increasing the high operational temperature in terms of the impact on the final product.

ACKNOWLEDGMENTS

The authors would like to acknowledge the support and collaboration of the Solar Committee of Chile, which was the main promoter of this study and to extend thank particularly to Ana Maria Ruz for her valuable contribution to the publication of this paper.

REFERENCES

1. Desierto de Atacama. *Comité Solar* (2017). Available at: http://www.comitesolar.cl/comite-solar/desierto-de-atacama/. (Accessed: 24th August 2018)
2. Coordinador Electrico Nacional » Reporte anual. Available at: https://www.coordinador.cl/informe-documento/reportes/731-2/. (Accessed: 24th August 2018)
3. Reporte Mensual y Reporte ERNC Sector Energético Julio 2018. Available at: https://www.cne.cl/2018/01/21/reporte-mensual-julio-2016-sector-energetico/. (Accessed: 24th August 2018)
4. Global Initiatives. *Comité Solar* (2017). Available at: http://www.comitesolar.cl/english/solar-road-map/global-initiatives/. (Accessed: 24th August 2018)
5. Kumar, R. A critical review on energy, exergy, exergoeconomic and economic (4-E) analysis of thermal power plants. *Engineering Science and Technology, an International Journal* **20,** 283–292 (2017).
6. Xu, C., Wang, Z., Li, X. & Sun, F. Energy and exergy analysis of solar power tower plants. *Applied Thermal Engineering* **31,** 3904–3913 (2011).
7. Modi, A. & Haglind, F. Performance analysis of a Kalina cycle for a central receiver solar thermal power plant with direct steam generation. *Applied Thermal Engineering* **65,** 201–208 (2014).
8. Soltani, R. *et al.* Multi-objective optimization of a solar-hybrid cogeneration cycle: Application to CGAM problem. *Energy Conversion and Management* **81,** 60–71 (2014).
9. Toro, C., Rocco, M. V. & Colombo, E. Exergy and thermoeconomic analyses of central receiver concentrated solar plants using air as heat transfer fluid. *Energies* **9,** 885 (2016).
10. Gómez-Hernández, J., González-Gómez, P. A., Briongos, J. V. & Santana, D. Influence of the steam generator on the exergetic and exergoeconomic analysis of solar tower plants. *Energy* **145,** 313–328 (2018).
11. Gallardo. "Factores Críticos para el desarrollo CSP en el desierto de Atacama". *Comité Solar* (2017). Available at: http://www.comitesolar.cl/english/documents/. (Accessed: 24th August 2018)
12. Ministerio de Energía - Planificación Estratégica. Available at: http://pelp.minenergia.cl/informacion-del-proceso/insumos-para-proyecciones. (Accessed: 24th August 2018)
13. Energia, S. I.-C. N. Precio Medio de Mercado - Comisión Nacional de Energía.
14. Kotas, T. J. The Exergy Method of Thermal Plant Analysis. (Elsevier, 2013).
15. Szargut, J. Exergy Method: Technical and Ecological Applications. (WIT Press, 2005).
16. Bejan, A., Tsatsaronis, G. & Moran, M. *Thermal design and optimization*. (John Wiley & Sons, 1996).
17. Bell, I. H., Wronski, J., Quoilin, S. & Lemort, V. Pure and Pseudo-pure Fluid Thermophysical Property Evaluation and the Open-Source Thermophysical Property Library CoolProp. *Ind. Eng. Chem. Res.* **53,** 2498–2508 (2014).
18. Leiva-Illanes, R., Escobar, R., Cardemil, J. M. & Alarcón-Padilla, D.-C. Comparison of the levelized cost and thermoeconomic methodologies – Cost allocation in a solar polygeneration plant to produce power, desalted water, cooling and process heat. *Energy Conversion and Management* **168,** 215–229 (2018).